Colloid Polym Sci (2009) 287:435–441
DOI 10.1007/s00396-008-1985-9

ORIGINAL CONTRIBUTION

Electrorheological characteristics of polyaniline/titanate composite nanotube suspensions

Qilin Cheng · Vladimir Pavlinek · Ying He · Chunzhong Li · Petr Saha

Received: 23 September 2008 / Revised: 26 November 2008 / Accepted: 10 December 2008 / Published online: 3 January 2009

Abstract In this paper, one-dimensional polyaniline/titanate (PANI/TN) composite nanotubes were synthesized by in situ chemical oxidative polymerization directed by block copolymer. These novel nanocomposite particles were used as a dispersed phase in electrorheological (ER) fluids, and the ER properties were investigated under both steady and dynamic shear. It was found that the ER activity of PANI/TN fluids varied with the ratio of aniline to titanate, and the PANI/TN suspensions showed a higher ER effect than that made by sphere-like PANI/TiO_2 nanoparticles. These observations were well interpreted by their dielectric spectra analysis; a larger dielectric loss enhancement and a faster rate of interfacial polarization were responsible for a higher ER activity of nanotubular PANI/TN-based fluids.

Keywords Electrorheological fluid · Polyaniline · Titanate nanotubes · Nanocomposite · Dielectric properties

Introduction

Over the past few years, controlled synthesis of nanomaterials with specific size and morphology has been the focus of considerable research in the field of materials science because their intrinsic chemical and physical properties can be effectively tuned by the morphology (e.g., dimensionality and shape) [1]. In particular, 1D nanoscale building blocks (nanotubes, nanowires, nanorods, and nanofibers) have currently received increased attention due to their unique properties and potential applications in nanodevices, optoelectronic devices, and chemical sensors [2–4]. Meanwhile, it is known that 1D nanostructured materials used as electrorheological (ER) fluids have been also recently reported to show interesting ER properties [5–7].

ER fluids are commonly known as suspensions consisting of particles with a high dielectric constant and low conductivity dispersed in an insulating liquid medium whose rheological properties can rapidly and reversibly change upon application of an external electric field [8–10]. The polarizable particles can attract each other to form chain or column structures spanning the electrode gap along the direction of the electric field; the suspensions undergo a rapid transition from a liquid state to a solid state within a millisecond under an electric field. This dramatic change caused by external electric field makes ER fluids ideal for a wide range of potential applications in mechanical engineering [10, 11]. Although various studies have been performed on ER materials until now, the experiment results are still far from their commercialization because of insufficient yield stress and large sedimentation. As a consequence, much effort must be devoted to developing effective ER fluids after overcoming such limitations.

Following this purpose, many advanced materials such as inorganic nanomaterials [12, 13], polymers [14, 15], conducting polymers and their nanocomposites [16–19], as well as novel nanomaterials with core–shell structure [20–22] have been developed to improve the ER performance. Among these materials, particular attention has been

Q. Cheng · V. Pavlinek (✉) · P. Saha
Polymer Centre, Faculty of Technology,
Tomas Bata University in Zlín,
TGM 275,
762 72 Zlín, Czech Republic
e-mail: pavlinek@ft.utb.cz

Q. Cheng · Y. He · C. Li (✉)
Key Laboratory for Ultrafine Materials of Ministry of Education,
School of Materials Science and Engineering,
East China University of Science and Technology,
200237 Shanghai, China
e-mail: czli@ecust.edu.cn

recently paid to 1D nanomaterials due to their potential advantages as dispersed phase for ER fluids including good suspended stability and possibly enhanced ER activity from relatively large aspect ratios or high surface areas. Despite many studies on the preparation of 1D nanomaterials, only a few studies [5–7] dealing with ER properties of 1D nanomaterial-based fluids have been reported so far.

In this paper, as a continuation of our brief previous report [23], we synthesized a novel 1D polyaniline/titanate composite nanotubes in which titanate (TN) nanotubes are the core and polyaniline (PANI) is the shell. The PANI/TN nanotubes may exhibit improved chemical and physical properties over individual components. Therefore, the potential application of PANI/TN as an ER fluid under both steady and dynamic shear is evaluated. A comparable study on ER effect between PANI/TN and PANI/TiO_2 fluids and their related dielectric properties is also investigated. The major aim of this paper was to provide a possible approach to the design of new ER materials through further study on ER behavior of 1D nanomaterials.

Experimental

Materials

Aniline (99%, Aldrich, USA) was distilled under reduced pressure. Ammonium persulfate [APS, $(NH_4)_2S_2O_8$, 98%] and the triblock copolymer poly (ethylene oxide)-poly (propylene oxide)-poly(ethylene oxide) (Pluronic P123, $EO_{20}PO_{70}EO_{20}$, M_w=5,800) were purchased from Aldrich Chemicals Company. TiO_2 powder (Degussa P25, Germany) was used as received without further treatment.

Synthesis of PANI/TN composite nanotubes

TN nanotubes were prepared according to the report [24], with a minor modification. In a typical synthesis, 1 g of TiO_2 powder was mixed with 60 ml of 10 M NaOH solution, which was followed by hydrothermal treatment of the mixture at 160 °C in a 100 ml Teflon-lined autoclave for 24 h. The white precipitate was separated by filtration and washed with distilled water until ~pH 7 was reached. The samples (TN nanotubes) were then dried in an oven at 60 °C for 12 h.

To obtain PANI/TN composite nanotubes, P123 (2 g) and TN nanotubes (0.5 g) were added to deionized water (50 ml) and ultrasonicated for 2 h to form a well-dispersed suspension and then cooled to 0–5 °C. A pre-cooled solution of aniline (An) monomer (mass ratio of An to TN was 1:1 and 2:1, respectively) was introduced into the equilibrated suspension drop by drop, and the mixture was further equilibrated at 0–5 °C for 2 h with constant mechanical stirring. Finally, the pre-cooled solution of APS was added dropwise to the aforementioned mixture, and the mixture was allowed to react in an ice bath for 24 h. The resulting precipitate was filtered and washed with distilled water and ethanol and then dried in a vacuum oven at 60 °C for 24 h. In addition, PANI/TiO_2 nanocomposite particles (mass ratio of An to TiO_2 was 2:1) were also prepared under the same synthetic conditions for comparison.

The morphologies of the materials were determined using a JEM 2100 F high-resolution transmission electron microscope and a JEOL 1200 transmission electron microscope (TEM). Fourier transform infrared (FTIR) spectra of the samples were obtained on Nicolet Magna-550 spectrometer in the range of 4,000–400 cm^{-1}.

Preparation of ER fluids

For the preparation of the suspensions, PANI/TN-1 (An/TN=1), PANI/TN-2 (An/TN=2), and PANI/TiO_2 (An/TiO_2=2) were treated with 3 vol.% NH_4OH solution to reduce the surface conductivity of the particles. Afterwards, the dried particles were dispersed by ultrasonic mixing in silicone oil (Fluid 200, Dow Corning, UK; viscosity η_c=108 mPa s, density d_c=0.965 g/cm^3) to form a stable suspension with a particle volume fraction of 5% (*v*/*v*) for each material separately.

Electrorheological and dielectric measurements

Measurements of rheological properties of the prepared fluids were carried out under controlled shear rate and controlled shear stress (CSS) mode using a coaxial cylinder viscometer (Bohlin GEMINI, Malvern Instruments, UK). The suspensions were placed in the Couette cell with the rotating inner cylinder of 14 mm in diameter and the outer cylinder separated by a 0.7-mm gap. They were connected to a DC power supply producing the following field strength: E=0.5–3 kV mm^{-1}. All the experiments were carried out at the temperature of 25 °C in the shear rate range 0.1–700 s^{-1}. Static yield stress was obtained from measurements performed in CSS mode. Further, dynamic viscoelastic tests were performed through dynamic strain sweeps and frequency sweeps. The strain sweep was carried out with applied strains of 10^{-4} to 1.0 at a frequency of 62.8 rad/s under an electric field in order to determine the linear viscoelastic region. The rheological parameters were then obtained from the frequency sweep tests (0.5 to 100 rad/s) at a fixed strain amplitude in the linear viscoelastic region.

Dielectric properties in the frequency range of 10^1–10^5 Hz were measured with a Hioki 3522 RCL Tester, Hioki, Japan. All experiments were performed at 25 °C.

Results and discussion

Material characteristic

The morphologies of PANI/TN-1, PANI/TN-2, and PANI/TiO_2 nanocomposites characterized by TEM are shown in Fig. 1. As can be seen, PANI/TN nanoparticles are tubular with the diameters in the range of 15–20 nm and lengths of up to several hundreds of nanometers (Fig. 1a, b). In contrast to them, PANI/TiO_2 nanoparticles are nearly sphere-like with a diameter of 100 nm (Fig. 1c). Apparently, the aspect ratios of PANI/TN composite nanotubes are around 15–20 times larger than that of PANI/TiO_2 composite nanoparticles.

The chemical structure of PANI/TN composite nanotubes was also investigated using FTIR spectroscopy. Both PANI/TN-1 and PANI/TN-2 composites show similar FTIR characteristic bands to those of polyaniline in the 1,000- to 1,600-cm^{-1} range, i.e., 1,590-, 1,496-, 1,302-, and 1,140-cm^{-1} bands. These characteristic bands can be related to the aromatic C=C stretching of quinonoid and benzenoid structures, C–N stretching mode for the benzenoid ring, and the electronic-like absorption of N=Q=N (Q represents the quinonoid ring), respectively [25]. Combined with TEM images, we can deduce that PANI is coated on the surface of TN nanotubes to form the composite nanotubes with core–shell structure.

Rheological properties of ER suspensions under steady shear

Figure 2 shows the flow behavior for both composite nanotube-based fluids under different electric field strengths. Without an electric field, both fluids show a slight deviation from the Newtonian fluid. In the presence of an electric field, the shear stress increases abruptly, showing a yield behavior of a Bingham fluid, and the viscosity exhibits a strong shear thinning behavior (Fig. 2c, d). Meanwhile, the shear stress and shear viscosity of both fluids increase with an increasing electric field strength at the same shear rate. However, it is worth noting that the shear stress exhibits either a slightly decreasing region ($E \leq$ 2 kV/mm) or a plateau region (E=3 kV/mm) over the broad range of shear rates (Fig. 2a, b). These phenomena are mainly associated with the change of microstructure of chains formed by polarized PANI/TN particles in silicone oil. Under an electric field, the electrostatic forces cause the dispersed PANI/TN particles to form chains or columns along the electric field direction; the reformation and destruction rate of particle chains depend on the competition between electrostatic and hydrodynamic forces [26, 27]. In particular, at higher electric field (e.g., E=3 kV/mm), the stronger electrostatic forces make the particle chains stiffer to maintain constant shear stress at low shear rates.

Figure 3 presents the dependence of static yield stress on the electric field strength for three ER fluids under the CSS mode. The yield stress increases with the electric field strength because of an increase in the dipole–dipole interaction among polarized particles. In general, the correlation of the yield stress, τ_y, with the electric field strength, E, at a fixed concentration is described as $\tau_y \propto E^{\alpha}$. The magnitude of exponent α is obtained by the linear fit of the relation of log $(\tau_y) \propto \alpha$ log(E) (shown in Fig. 3). The α values for PANI/TN-1 and PANI/TN-2 suspensions are 1.819 and 1.820, respectively, which deviate from the theoretical prediction by the polarization model [28] for a well-developed structure (α=2), while that for PANI/TiO_2 fluid is around 2. The α values for PANI/TN ER fluids are almost the same, suggesting that the amount of TN in composite nanotubes is not the main factor influencing the value of exponent α. On the contrary, the deviation is

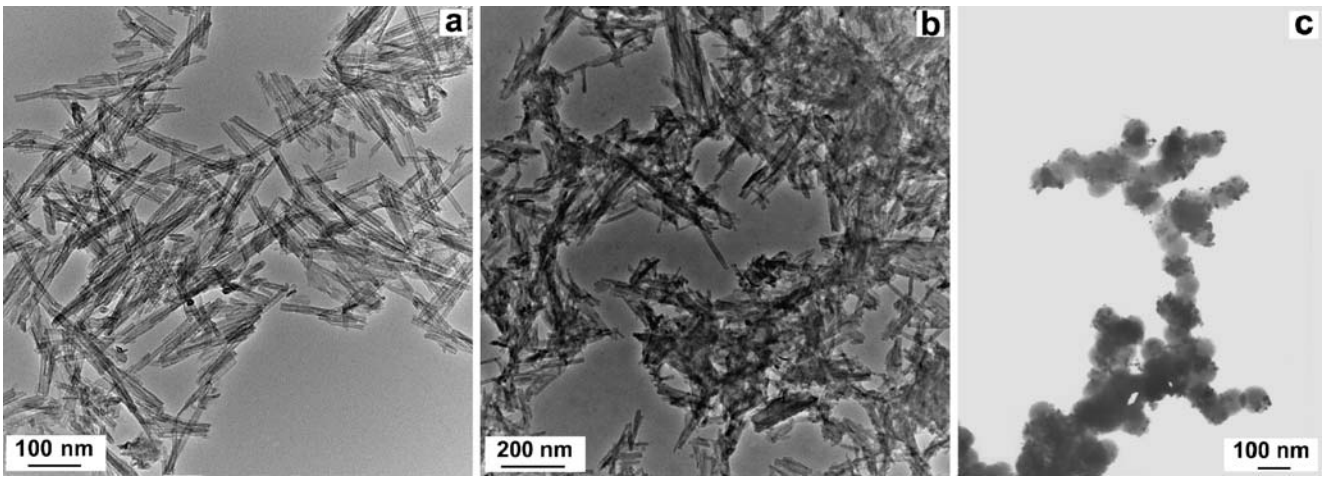

Fig. 1 TEM images of PANI/TN-1 (**a**), PANI/TN-2 nanotubes (**b**), and PANI/TiO_2 nanoparticles (**c**)

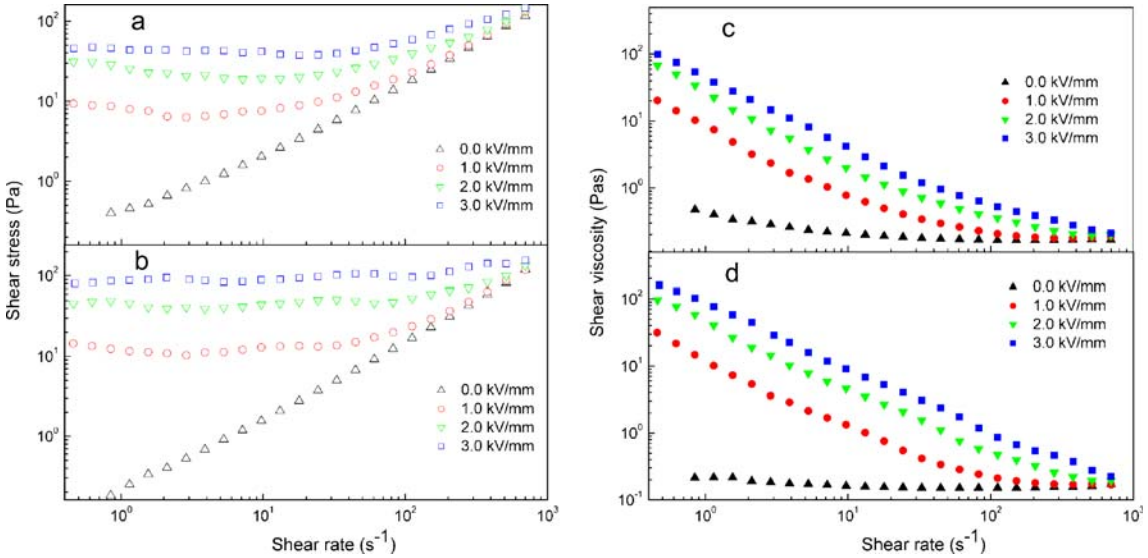

Fig. 2 Flow curves for PANI/TN-1 (**b**, **d**) and PANI/TN-2 (**a**, **c**) based fluids under different electric field strengths

caused by the electric field strength, the concentration and shapes of particles [29]; however, in this study, the structural peculiarity of PANI/TN nanocomposites may be the main factor. This nonlinear ER behavior ($\tau_y \propto E^{\alpha}$, $\alpha<2$) has also been reported in the case of other conducting polymer-based suspensions [30, 31].

To develop a better understanding of the TN doping degree and the shape of particles on the ER effect of fluids, ER efficiency as a function of E for three fluids is plotted in Fig. 4. For practical applications of the ER fluids, the ER efficiency is determined by $(\tau_E - \tau_0)/\tau_0$, where τ_E andτ_0 are the shear stresses with and without electric field at low shear rate (0.4 s^{-1}). This ratio determines a relative increase in the shear stress induced by an electric field. Apparently, the ER efficiency for three fluids increases with E, and the ER efficiency for PANI/TN-1 is significantly higher than that of PANI/TN-2 fluid in the range of E=0–3 kV/mm. Because both materials are nanotubes with a core–shell structure in which the polyaniline is deposited on the surface of titanate nanotubes, the thickness of PANI layer for PANI/TN-2 could be larger than that for PANI/TN-1 due to a different ratio of An to TN. A different thickness of the conducting polymer shell can result in a change in the polarization rate induced by the electric field [27, 32]. On the other hand, the sphere-like PANI/TiO_2 fluid shows the lowest ER efficiency. This different phenomenon will be discussed further on the basis of dielectric spectra analysis.

Dynamic viscoelasticity

A dramatic change of an ER fluid microstructure under an applied electric field is reflected in a rapid transition from Newtonian liquids to rigid solids. When a shear strain is small enough, the ER fluid demonstrates elastic properties. To investigate such behavior of solidified fluids under an applied electric field, dynamic oscillation tests were also performed. In dynamic tests, storage, G' and loss, G'', moduli are often used to describe the change of the

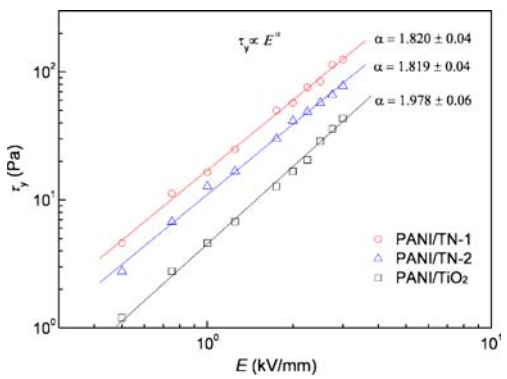

Fig. 3 Static yield stress versus the electric field strength for PANI/TN-1, PANI/TN-2, and PANI/TiO_2 ER fluids

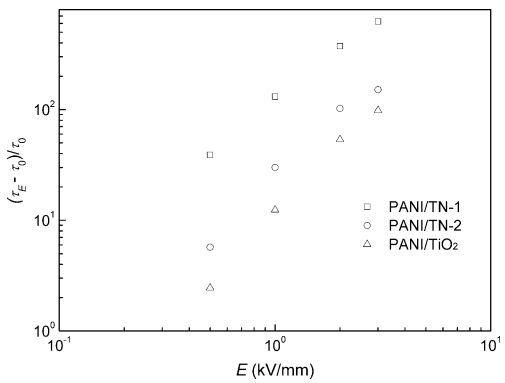

Fig. 4 ER efficiency of PANI/TN-1 and PANI/TN-2 ER fluids versus the electric field strength at the shear rate of 0.4 s^{-1}

suspension microstructures. As a representative of PANI/TN fluids, the strain dependence of G' and G'' for PANI/TN-2 fluid under various electric field strengths is shown in Fig. 5. As can be seen, in the linear viscoelastic region, G' is larger than G''; meanwhile, the linear viscoelastic region varies with the increasing electric field strength. Since G' depends on field-induced interactions among PANI/TN-2 particles, the strong interactions and the stiff chain structure thus contribute to large G'. Upon application of an electric field, the PANI/TN-2 particles form chains spanning the gap between the electrodes. These chains become more stable and stiffer with the increasing electric field strength, and thus, the fluid is solidified and showing elasticity. Therefore, in the linear viscoelastic region, G' dominates over G''; however, as the strain increases, the chain structures continuously undergo large deformations and a rupture beyond a certain degree of deformation takes place. Finally, the system starts to flow, showing prevailing viscous behavior (i.e., $G''>G'$) [33].

Figure 6 shows the strain dependence of G' and G'' for PANI/TN-1, PANI/TN-2, and PANI/TiO_2 fluids at an electric field strength of 2 kV/mm. In the presence of an electric field, each suspension shows solid-like behavior ($G'>G''$), and G' for PANI/TN-1 is the largest in the linear viscoelastic region and its corresponding G'' displays a similar trend. This can be explained by the stiffest chain structures being formed by polarized PANI/TN-1 particles in an imposed electric field, which results in the highest rigidity demonstrating the largest modulus. Figure 7 presents G' for three fluids as a function of frequency at a small strain of 2×10^{-4} in the linear viscoelastic region. Without an electric field, G' for three fluids is dependent on frequency, whereas it increases significantly over a wide frequency range upon an electric field. At low frequency, G' for three fluids exhibits very little dependence on frequency due to predominant elasticity, and at the same electric field strength, G' for PANI/TN-1 fluids is the highest. The results indicate

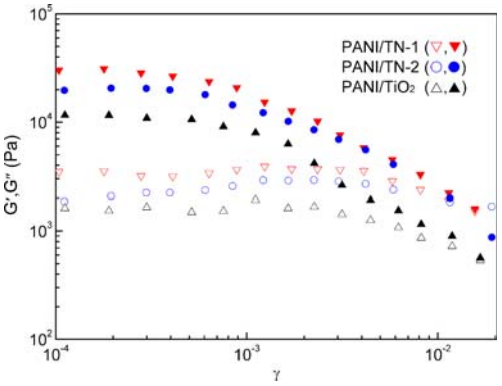

Fig. 6 Strain dependence of G' and G'' for PANI/TN-1, PANI/TN-2, and PANI/TiO_2 fluids at E=2 kV/mm. *Solid symbols* for G'; *open symbols* for G''

that the strongest interactions among PANI/TN-1 particles lead to the highest rigidity of their chain structures, as revealed by the largest G'.

It is well known that the ER performance of an ER fluid depends not only on the electric field strength, dielectric properties, and the particle volume fraction but also on the particle shape. Qi and Wen [34] proposed that microsphere-based fluid showed a better ER performance than microrod-based fluid, and the particle aspect ratio had little influence on the ER effect of an anhydrous ER fluid. However, recent studies [5, 35] indicate that whisker fluid exhibits a higher ER activity than spherical-particle-based fluid. In our study, the nanotubular PANI/TN-based fluids also exhibit a higher ER activity than the sphere-like PANI/TiO_2 fluid. The possible reasons may lie in two aspects: Firstly, the particle chains are more easily developed from tubular rather than sphere-like nanoparticles even though the particle concentration is low [36]; secondly, particles with a great diversity of structure give rise to different polarization under an applied electric field. This mechanism related to the rate of polarization will be discussed below.

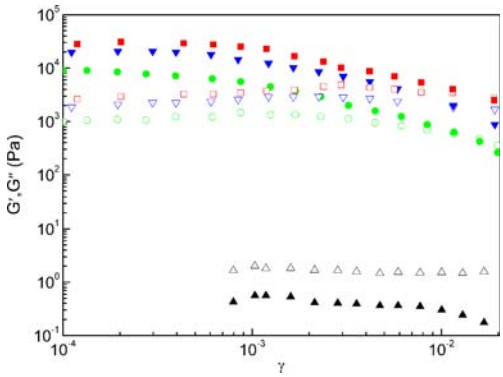

Fig. 5 Strain dependence of G' (*solid symbols*) and G'' (*open symbols*) for PANI/TN-2 fluid under various E (kV/mm): 0 (*triangles*), 1 (*circles*), 2 (*inverted triangles*), 3 (*squares*)

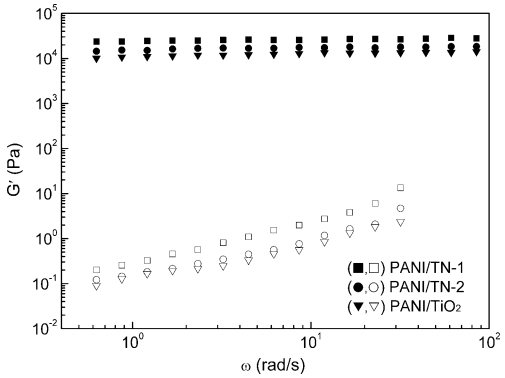

Fig. 7 Frequency dependence of G' for PANI/TN-1, PANI/TN-2, and PANI/TiO_2 fluids at different E: 0 kV/mm (*open symbols*); 2 kV/mm (*solid symbols*)

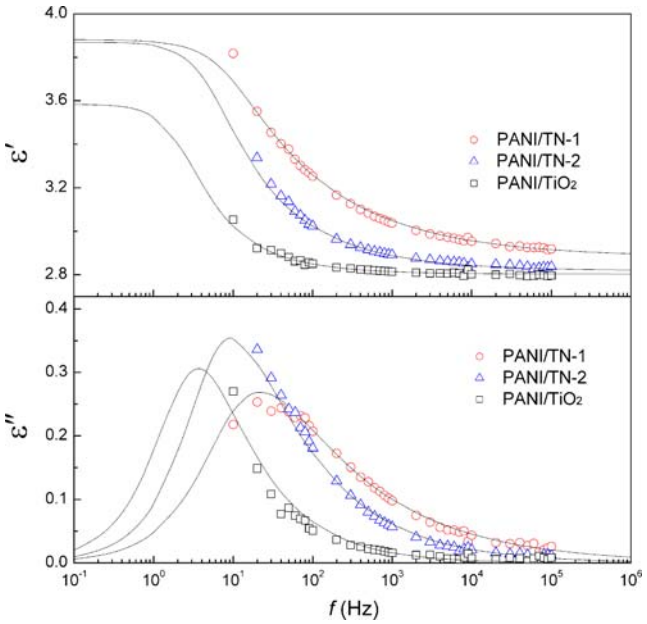

Fig. 8 Dependence of relative permittivity ε' and dielectric loss factor ε'' on frequency for PANI/TN-1, PANI/TN-2, and PANI/TiO_2 suspensions

Dielectric properties of suspensions

The particle polarization is believed to be a crucial factor in the generation of the ER effect. According to a widely accepted interfacial polarization mechanism proposed in [37–40], a good ER effect requires that ER fluids have a proper ε'' dielectric relaxation peak in the range of 10^2–10^5 Hz and a large polarizability, $\Delta\varepsilon'\left(\Delta\varepsilon' \approx \varepsilon_0' - \varepsilon_\infty'\right)$, where ε_0' and ε_∞' are relative permittivity extrapolated to zero and infinite frequency, respectively. The proper ε'' peak position and large $\Delta\varepsilon'$ do not only result in increased interactions between particles but also maintain a stable chain structure formed by particles under applied electric and shear fields [41]. Figure 8 shows the dielectric spectra of PANI/TN-1, PANI/TN-2, PANI/TiO_2 suspensions where lines represent the fits of the Havriliak–Negami equation [42].

$$\varepsilon^* = \varepsilon' + i\varepsilon'\prime = \varepsilon_\infty' + \frac{\varepsilon_0' - \varepsilon_\infty'}{\left(1 + (2\pi f\lambda i)^\beta\right)^m}. \quad (1)$$

Here, λ is the relaxation time reflecting the rate of interfacial polarization, β determines the scattering degree of relaxation time while m is related to the asymmetry of relaxation time spectrum, and $\Delta\varepsilon'$ shows the degree of polarization induced by an electric field. The parameters in Eq. 1 for three ER fluids are given in Table 1. It is obvious that only a dielectric loss peak of the PANI/TN-1 suspension is observed, indicating a relatively stronger interfacial polarization. On the other hand, based on the fitting results, the $\Delta\varepsilon'$ values for PANI/TN-1 and PANI/TN-2 are similar but larger than those for the PANI/TiO_2-based fluid. The relaxation time, λ, increases in the same sequence. Note that $\Delta\varepsilon'$ shows the degree of polarization corresponding to the electrostatic interactions between particles and λ reflects the rate of interfacial polarization related to the stress increase during deformation [14]. Smaller $\Delta\varepsilon'$ and longer λ fluid result in a weak ER effect for the PANI/TiO_2 fluid. Although the $\Delta\varepsilon'$ values for PANI/TN-1 and PANI/TN-2 fluids are almost the same, the shorter λ of the PANI/TN-1 fluid produces a faster polarization rate than that of the PANI/TN-2 fluid under an electric field, which leads to stronger and stiffer chain structures being formed by PANI/TN-1 particles. Therefore, PANI/TN-1 shows the comparatively highest ER activity among all three fluids compared.

Conclusions

New anhydrous ER fluids with polyaniline/titanate (PANI/TN) composite nanotubes dispersed in silicone oil were investigated. The ER fluids of PANI/TN exhibit typical ER characteristics and their ER properties vary with the amount of TN. The tubular structure with a large aspect ratio may result in a stronger polarizability of PANI/TN particles in ER fluids under an applied electric field, which gives rise to a higher ER activity than that of sphere-like PANI/TiO_2. These ER characteristics were analyzed via the dielectric spectra of ER fluids. Viscoelastic measurements also indicate that the storage modulus is larger than the loss modulus in the linear viscoelastic region, and the chain structures formed by polarizable particles become more elastic and stiffer with increasing electric field strength. The results of this study

Table 1 Parameters in Eq. 1 of three ER fluids

Dispersed phase	ε_s'	ε_∞'	$\Delta\varepsilon' = \varepsilon_s' - \varepsilon_\infty'$	λ (s)	β	m
PANI/TiO_2	3.583	2.803	0.781	0.066	1.0	0.613
PANI/TN-2	3.869	2.819	1.05	0.031	1.0	0.461
PANI/TN-1	3.882	2.882	1.00	0.017	0.921	0.376

will be helpful both in the further elucidation of ER behavior of 1D nanomaterials-based fluids and in the design of high-performance ER materials.

Acknowledgments This work was supported by the Ministry of Education, Youth and Sports of the Czech Republic (MSM 7088352101) and the Grant Agency of the Czech Republic (202/06/0419). The authors also wish to thank to the National Natural Science Foundation of China (20236020), the National High Technology Research and Development Program of China (2006AA03Z358), and 973 Program (2004CB719500) for their financial support.

References

1. Burda C, Chen X, Narayanan R, El-Sayed MA (2005) Chem Rev 105:1025
2. Law M, Sirbuly DJ, Johnson JC, Goldberger J, Saykally RJ, Yang P (2004) Science 305:1269
3. Li ZF, Swihart MT, Ruchenstein E (2004) Langmuir 20:1963
4. Huang Y, Duan XF, Lieber CM (2005) Small 1:142
5. Ying JB, Zhao XP (2006) Nanotechnology 17:192
6. Lozano K, Hernandez C, Petty TW, Sigman MB, Korgel B (2006) J Colloid Interface Sci 297:618
7. Feng P, Wan Q, Fu XQ, Wang TH, Tian Y (2002) Appl Phys Lett 87:033114
8. Block H, Kelly JP (1998) J Phys D Appl Phys 21:1661
9. Klingenberg DJ, Zukoki CF (1990) Langmuir 6:15
10. Hao T (2001) Adv Mater 13:1847
11. Tian ZJ, Zou XW, Zhang WB, Jin ZZ (1999) Phys Rev E 59:3177
12. Liu Y, Liao FH, Li JR, Zhang SH, Chen SM, Wei CG, Cao S (2006) Scripta Mater 54:125
13. Wang BX, Zhao XP, Zhao Y, Ding CL (2007) Compos Sci Technol 67:3031
14. Sung JH, Jang WH, Choi HJ, Jhon MS (2005) Polymer 46:12359
15. Chiang YC, Jamieson AM, Kawasumi M, Perec V (1997) Macromolecules 30:1992
16. Lengalova A, Pavlinek V, Saha P, Quadrat O, Kitano T, Stejskal J (2003) Eur Polym J 39:641
17. Woo DJ, Suh MH, Shin ES, Lee CW, Lee SH (2005) J Colloid Interface Sci 288:71
18. Kim YD, Song IC (2002) J Mater Sci 37:5051
19. Cho MS, Choi HJ, Ahn WS (2004) Langmuir 20:202
20. Wen W, Huang X, Yang X, Lu X, Sheng P (2003) Nat Mater 2:727
21. Wang BX, Zhao XP (2005) Adv Mater 15:1815
22. Cheng Q, Pavlinek V, Lengalova A, Li C, He Y, Saha P (2006) Micropor Mesopor Mater 93:263
23. Cheng Q, Pavlinek V, He Y, Li C, Lengalova A, Saha P (2007) Eur Polym J 43:3780
24. Lan Y, Gao X, Zhu Y, Zheng Z, Yan T, Wu F, Ringer SP, Song D (2005) Adv Funct Mater 15:1310
25. Li CC, Zhang ZK (2004) Macromolecules 37:2683
26. Woo DJ, Suh MH, Shin ES, Lee CW, Lee SH (2005) J Colloid Interface Sci 288:71
27. Cho MS, Cho YH, Choi HJ, Jhon MS (2003) Langmuir 19:5875
28. Klingenberg DJ, Van Swol F, Zukoski CF (1991) J Chem Phys 94:6170
29. Davis LC (1997) J Appl Phys 81:1985
30. Yoon DJ, Kim YD (2006) J Colloid Interface Sci 303:573
31. Cho MS, Choi HJ, To K (1998) Macromol Rapid Commun 19:271
32. Pavlinek V, Saha P, Kitano T, Stejskal J, Quadrat O (2005) Physica A 353:21
33. Hiamtup P, Sirivat A, Jamieson AM (2006) J Colloid Interface Sci 295:270
34. Qi Y, Wen W (2002) J Phys D Appl Phys 35:2231
35. Tsuda K, Takeda Y, Ogura H, Otsubo Y (2007) Colloid Surface A 299:262
36. Kanu RC, Shaw MT (1998) J Rheol 42:657
37. Block H, Rattay P (1995) In: Havelka KO, Filisko FE (eds) Progress in electrorheology. Plenum, New York, p 19
38. Ikazaki F, Kawai A, Uchida K, Kawakami T, Edamura K, Sakura K, Anzai H, Asako Y (1998) J Phys D Appl Phys 31:336
39. Hao T, Kawai A, Ikazaki F (1998) Langmuir 14:1256
40. Hao T, Kawai A, Ikazaki F (1999) Langmuir 15:918
41. Yin JB, Zhao XP (2004) Chem Phys Lett 398:393
42. Havriliak S, Negami S (1966) J Polym Sci C 16:99